We are IntechOpen, the world's leading publisher of Open Access books Built by scientists, for scientists

6,900
Open access books available

186,000
International authors and editors

200M
Downloads

Our authors are among the

154
Countries delivered to

TOP 1%
most cited scientists

12.2%
Contributors from top 500 universities

WEB OF SCIENCE™

Selection of our books indexed in the Book Citation Index in Web of Science™ Core Collection (BKCI)

Interested in publishing with us?
Contact book.department@intechopen.com

Numbers displayed above are based on latest data collected.
For more information visit www.intechopen.com

23

Coupling Experiment and Nonlinear Numerical Analysis in the Study of Post-Buckling Response of Thin-Walled Airframe Structures

Tomasz Kopecki
Rzeszów University of Technology, Poland

1. Introduction

Rational approach to design of load-carrying structures seems to suggest the necessity of focusing special attention on crucial areas of these structures, which are decisive for durability and reliability of the structure. The presence of such crucial areas in a designed solution, resulting usually from its practical functions, should be given careful consideration in view of opportunity to introduce appropriate changes in the design solutions possibly before costly and time-consuming workshop realization of a prototype.

The intent of the author is to draw attention to gravity of the factor integrating nonlinear numerical analysis with an experiment – in a broad sense of this word. Then, this chapter presents a methodology that can be used for assessment and current improvement of numerical models thus ensuring correct interpretation of results obtained from nonlinear numerical analyses of a structure.

The proposed methodology is based on carrying out experimental examination of selected crucial elements of load-carrying structures parallel with their nonlinear numerical analysis. Special attention is paid to factors determining proper realization of adequate experiments with emphasis placed on the role which the model tests can play as a fast and economically justified research tool that can be used in the course of design work on thin-walled load-carrying structures.

The presented considerations are illustrated by an example structures, whose degree of complexity and deformation range is characteristic for modern solutions in the design of airframe load-carrying structures. As a representative part of the construction design, a fragment of a load-carrying structure containing an extensive cutout, in which the highest stress levels and gradients occur in the conditions of torsion resulting in post-buckling deformation states within the range of permissible loads, was selected. Stress distributions observed within that range of deformation constitute a basis for determination of the structure's fatigue life.

Research described in this chapter were carried out in two stages:

In first of them, the objects of research constituted open section cylindrical shells with relatively small diameter in comparison to the length. In this case, the point of analysis was the determination of critical loads values and forms of deformations of free edges of examined structures, which was devoid of reinforcements or reinforced with the stringers.

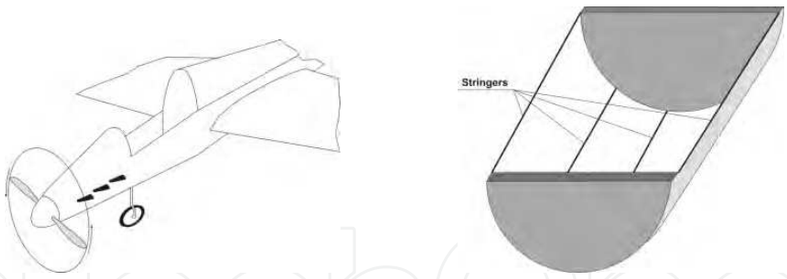

a) b)

Fig. 1. (a) an example of extensive cutout in the airframe structure;
(b) isolated, critical fragment of the structure

In the second stage of research, objects of research were the cylindrical shells reinforced with the stringers protected from the buckling thanks to their considerable geometrical moments of inertia. Special attention was focused on the problem of the loss of stability of the shells.

2. Post-buckling study of open section cylindrical steel shells subjected to constrained torsion

The subject to be considered concerned numerical-experimental analysis of open cross section thin-walled cylindrical shells, characterized by the relatively big ratio between length and diameter. The range of numerical calculations included post-buckling stress analysis and determination of critical loads. Two geometrically varied structures were considered. The first is an open section cylindrical shell without stiffening. The second structure represented the shell reinforced by three stringers in the closed section. Special attention was focused on the problem of buckling of the edge of the shell, which is tantamount to the collapse of the structure.

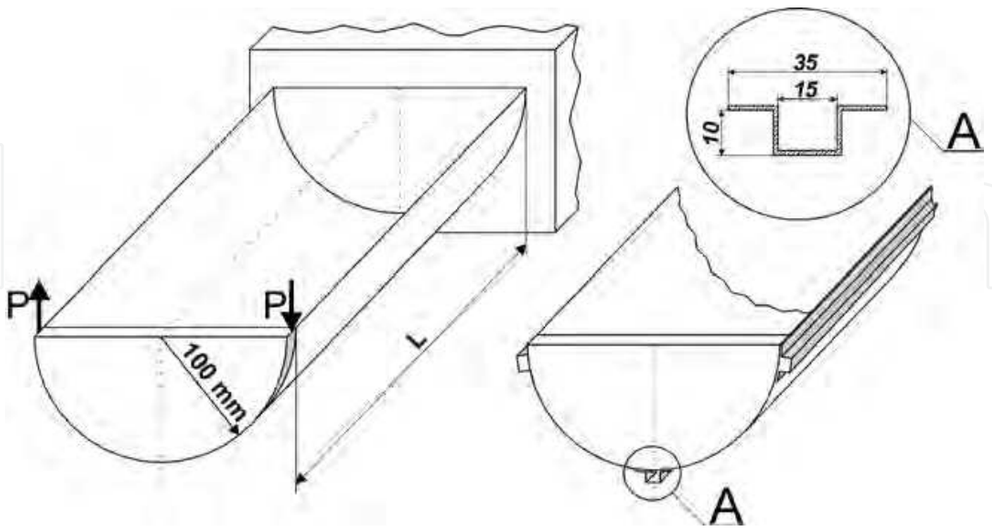

Fig. 2. Installation, loading device, and dimensions of the cross section.

Parallel to the numerical computations, for both two variants mentioned above, actual experiments were performed. A ratio of L/D=5 was assumed in both cases.

Experimental models were made of steel. The installation, loading device and structure dimensions with reinforcing stringers cross section is shown in Fig. 2.

2.1 Actual experiments

Parallel to the numerical calculations, qualitative experimental testing was performed on both variants of the structure. This provided a method for comparison of post-buckling shape and critical load values obtained in the numerical manner.

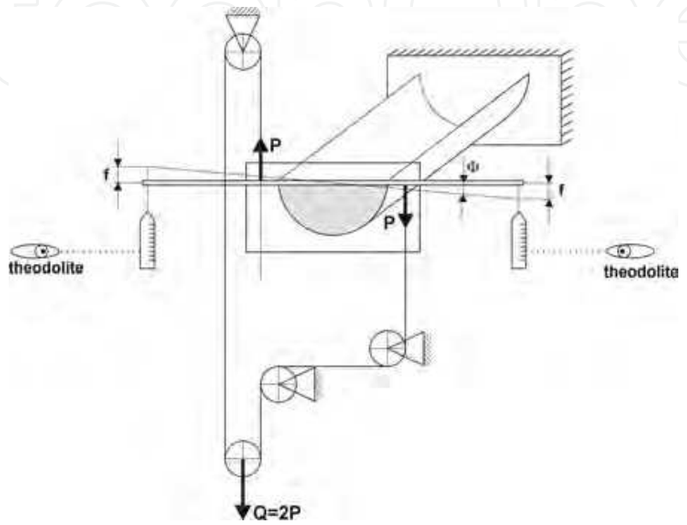

Fig. 3. The experiment device

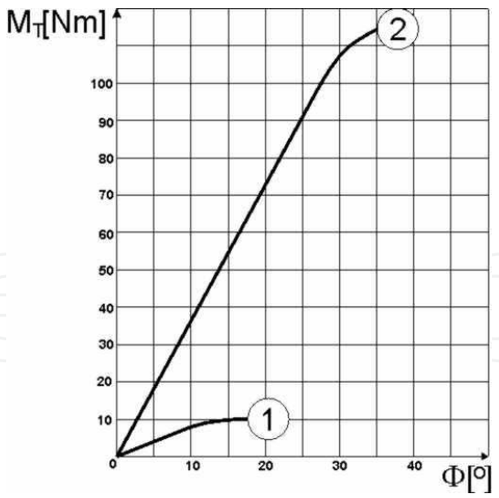

Fig. 4. Representative equilibrium path: torsion angle versus torque moment: 1 - shell without reinforcement, 2 - structure with stiffeners

The experiment was carried out on a special station able to provide the assumed loading and boundary conditions. Two cases were considered: the shell without reinforcement, and a structure with three stringers of closed section. In both cases the specimen length was L=1[m]. Figure 3 shows the design of this device.

The plot of torsion angle versus torsion moment, accepted as the representative equilibrium path, is shown by Fig. 4.
Fig. 4 shows, in the range of pre-buckling, that the load relationship between torsion moment and torsion angle is linear, exactly up to the moment of abrupt variation. Post-buckling forms of deformations are shown on fig.5 and fig.6.

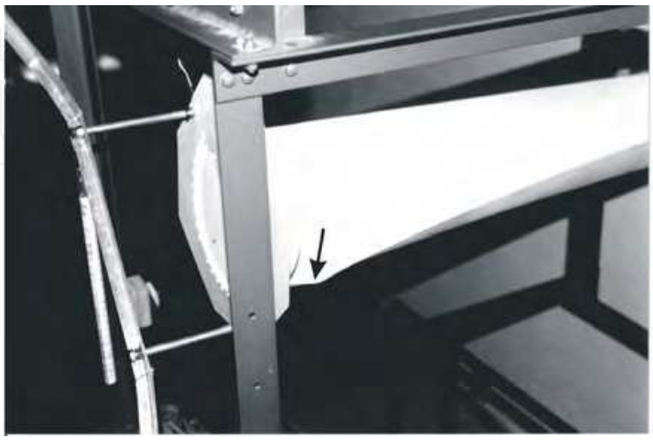

Fig. 5. Local buckling of the structure without reinforcement; L=1[m].

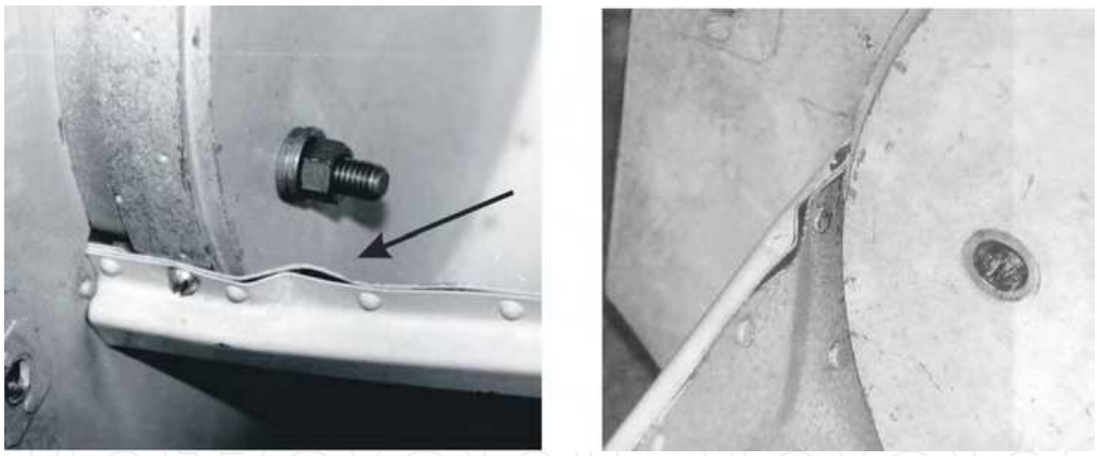

Fig. 6. Post-buckling plastic deformation. Structure reinforced by closed section stiffeners.

These experiments show that the structures considered are characterised not only by low torsional rigidity, but also by large deformations. Therefore application of the linear FEM analysis can only refer to the under-critical deformation range. It provides a way to identify stress concentration zones, possibly local buckling areas.
In order to determine the stress distribution in the post-buckling state, nonlinear static analysis was done. The stress-strain relation of uniaxial tension for actual material was simplified by the model of the ideal elastic - plastic body with a yield point of 240[MPa] (Fig.7).

2.2 Nonlinear FEM analysis

The results of the experiments showed that even a small load increment over the critical value leads to local plastic deformation. Numerical simulation of post-buckling deformation

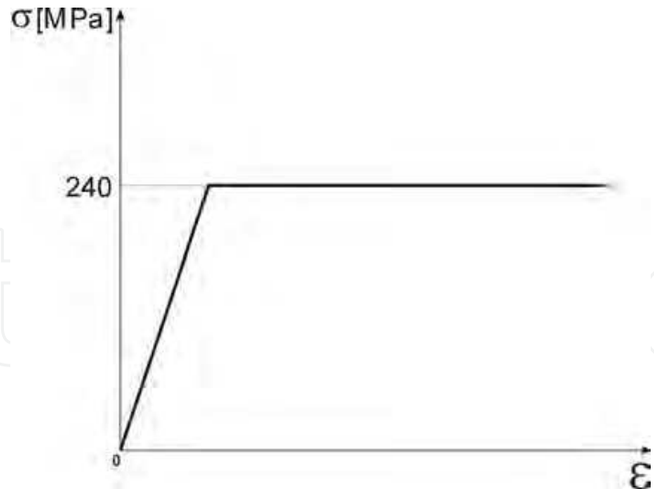

Fig. 7. Stress-strain relation of idealised material.

requires a nonlinear application. Large deformations and the change of the structure's rigidity have to be taken into consideration.

Nonlinear formulation of the problem is managed by the discrete equilibrium equations encountered in nonlinear static structural analysis, formulated by the displacement method presented in the compact force residual form

$$\mathbf{r}(\mathbf{u},\Lambda) = \mathbf{0}. \tag{1}$$

Here **u** is the state vector, containing the degrees of freedom that characterize the configuration of the structure; **Λ** is an array of control parameters, containing the components of external loading, whereas **r** is the residual vector containing out-of-balance forces conjugated to **u.** Varying the vector **r** with respect to the components of **u** in the assumption - **Λ=**constant, a tangent stiffness matrix **K** in a structural mechanics application can be written as:

$$K=\frac{\partial r}{\partial u}. \tag{2}$$

An alternative version of equation (1) is the force-balance form:

$$p(u)=f(u,\Lambda). \tag{4}$$

The **p** vector contains components of internal forces, resulting from deformation of the structure; however **f** are the control-dependent external forces, composing the set introduced respectively during the next stages of the analysis, which may also be dependent on the current geometry of the structure.

The philosophy of the nonlinear analysis in FEM is based on the gradual application of control parameters, completed in further stages. It corresponds to the stage for every reliable state of the structure in which a static balance is specific for a corresponding solution of equation (1). Control parameters connected to external force components are generally expressed as functions of reliable quantity **λ,** called the stage control parameter. The result of the nonlinear analysis composes a set of solutions, corresponding to each value of the **λ**

parameter. They create the equilibrium path of the system. The unambiguous graphical interpretation of the equilibrium path is possible for at most two degrees of freedom. However with the knowledge of external loading, the value of stage control parameters and related geometric structural configurations, it is possible to obtain an approximated dependence between selected values describing deformation of the structure versus external loading. For the numerical models considered, equilibrium paths were determined in the method: torsional moment versus total torsional angle.

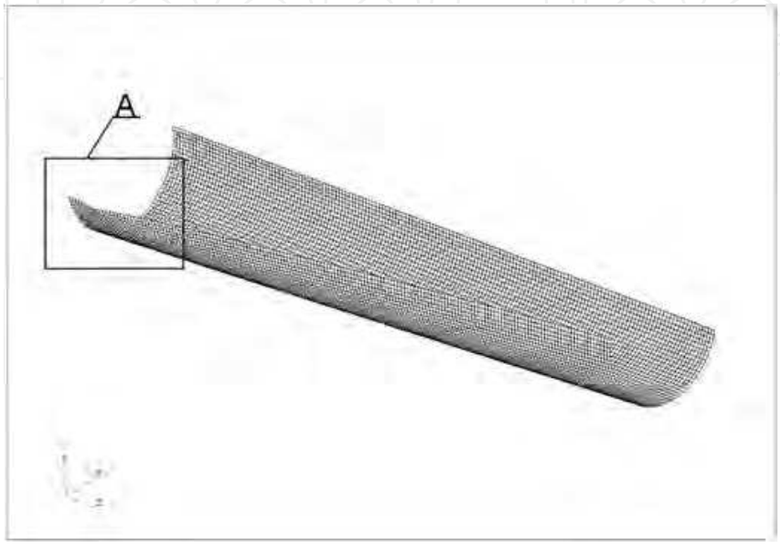

Fig. 8. Post buckling deformation. Structure without stringers

Algorithms of nonlinear analysis are mainly based on iterative and incremental - iterative procedures. The stiffness matrix **K** is treated in every equation stage as a constant and it is increased as far as the **λ** stage control parameter is increaded. The Newton-Raphson algorithm constitutes the basic iterative method. Its' drawback is that it cannot obtain the solution convergence. This method is bound up with the appearance of the limit of bifurcation points on the equilibrium path. In such situations the arc length method is applied, which makes it possible to determine the balance of the system.

Nonlinear numerical analyses of this problem were done applying the MSC MARC 2007 programme. This programme allows the user to intervene in the iteration parameter selection.

Two diversified numerical models were analyzed, with the structure stiffened by the stringers of "omega" in the cross section of each. The first has a surface - stringer rivet joint simulated by beam elements. Contact was also reflected between the surfaces of stringers and the surface itself. A simplification was applied in the second model, relying on the continuous connection of stringers with surface.

After several numerical tests, the boundary conditions of all models were changed, due to their excessive stiffness. The establishment of the back edges of the shells, as shown in Fig.1 was replaced by ribs with additional supports.

The effects illustrating the character of deformation in numerical calculations and effective stress distribution on external structural surfaces are shown by Figs. 8-13.

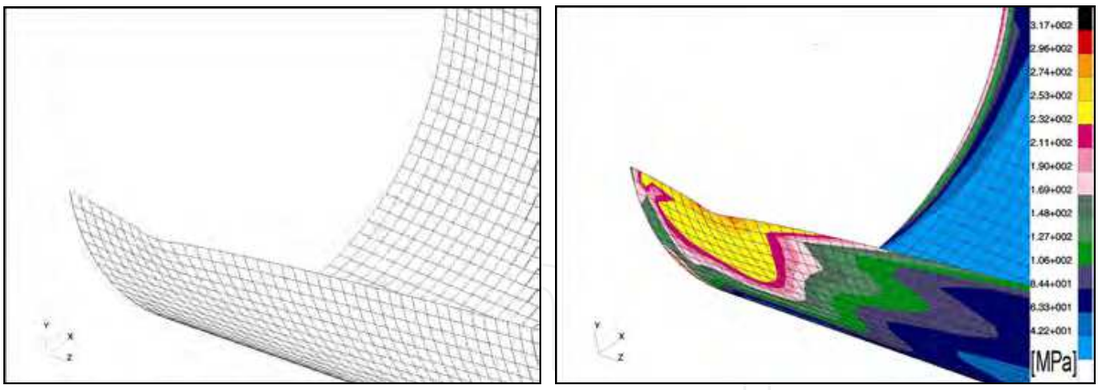

a) b)

Fig. 9. Form of post buckling deformation; a) area of A detail in actual scale; b) effective stress distribution on external surface according to von Mises' criterion.

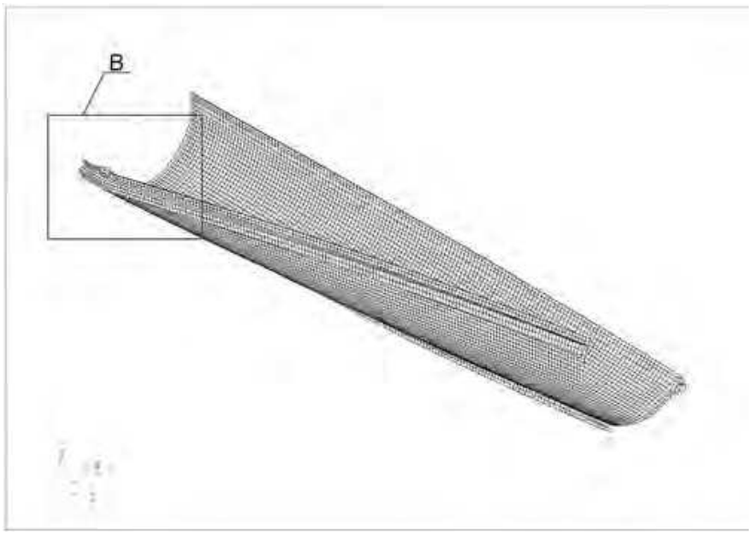

Fig. 10. Reinforced structure -version 1- riveted joint of the surface with the stringer. Local post-buckling deformation.

The results of the calculations presented in Figs. 8 and 9 prove the existence of local plastic deformation areas in the vicinity of the boundary fixing of the structure. These effects show satisfactory compatibility with the experiment (compare Fig. 5), both in the location and the character of the plastic deformation range.

Figures 10 and 11 show the numerical results for the model, where the connection was reflected by inner rivets. The result obtained, describing the state of local plastic deformation in a post-buckling state, differs qualitatively from the effect noted in the experiment.

Several attempts were made (not presented here) to identify reasons for this divergence. It is possible, on this basis, to make an attempt to explain this phenomena.

Looking at Fig. 11, we can notice that the elements of the surface and stringer in the zone between rivets were subjected to transverse dislocations moving in opposite directions, while the direction of dislocations were the same. This divergence could be the result of a loss of stability bifurcation. A reasonable suggestion arises from the fact that in both

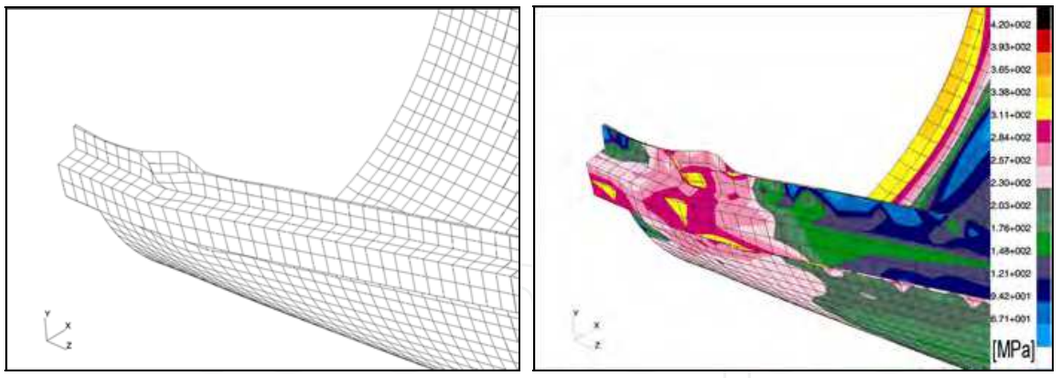

a) b)

Fig. 11. Form of post-buckling deformation; a) area of C detail in actual scale; b) effective stress distribution on external surface according to von Mises' criterion.

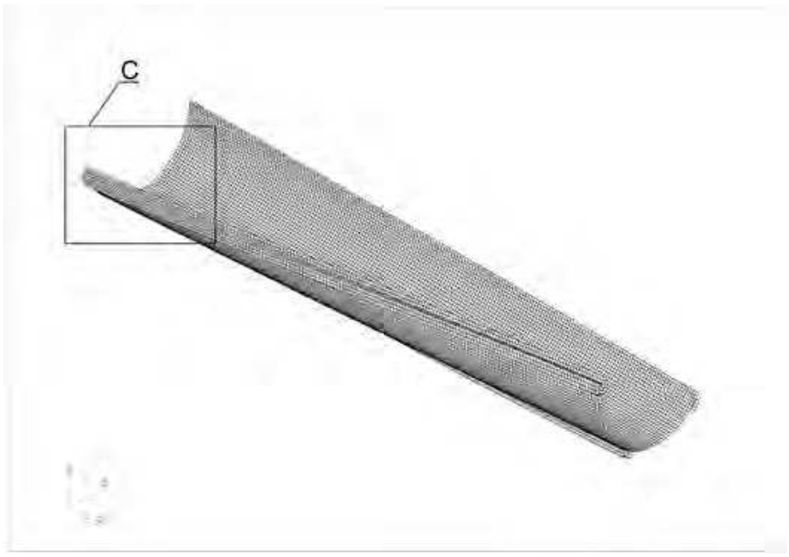

Fig. 12. Reinforced structure - version 2 - continuous connection of surface and stringers. Local post-buckling deformation.

elements the bifurcation had a stable-symmetrical character. In the actual structure, geometric imperfections could determine the identical direction of the dislocation of both surfaces already initiated during the riveting process.

The second model (Figs. 12-13) was of considerable interest. The results of numerical calculations correspond exactly to the results of the experiment (Fig. 6). Applied simplifications adjust conditions of the iteration parameters selection in the actual structure transformation. They rely on the continuous connection between stringers and surfaces which eliminates the possibility of local stress concentration in the proximity of the rivets. Taking into consideration the character of advanced plastic deformation as noted, and the responding stress distribution, it is possible to regard the results obtained as satisfactory.

In Fig. 14, the relationship between the torsion moment and the torsion angle is shown as obtained both in the experiment and in the calculation.

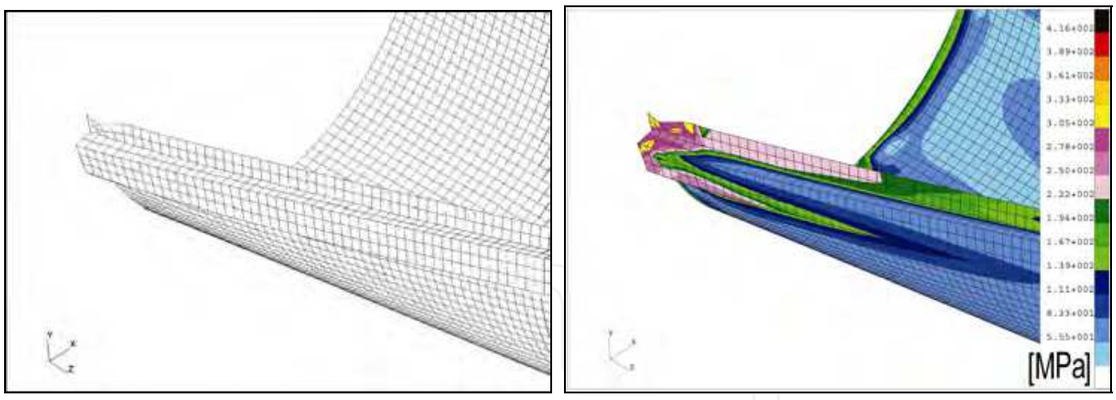

a) b)

Fig. 13. Form of post-buckling deformation; a) area of B detail in actual scale; b) effective stress distribution on the external surface according to von Mises' criterion.

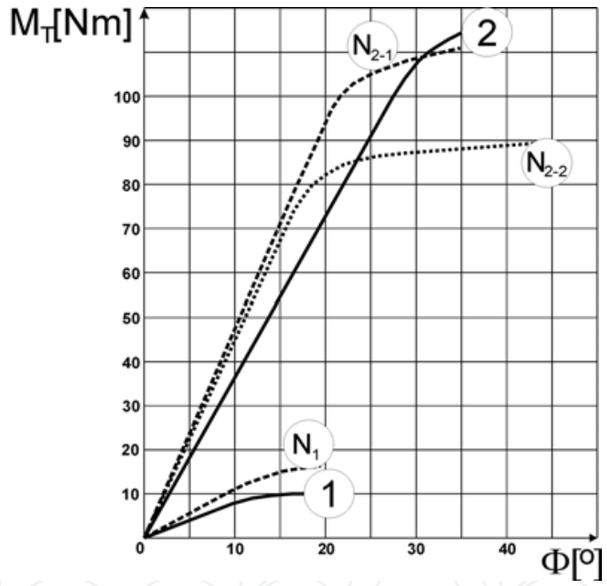

1 - Structure without stringers – experimental result
2 - Structure reinforced by closed section stiffeners – experimental result
N_1 - Structure without stringers – numerical result
$N_{2\text{-}1}$ - Version with continuous connection of surface and stringers – numerical results
$N_{2\text{-}2}$ - Version with riveted joint of the surface with the stringers – numerical results

Fig. 14. Relationship between the torsion moment versus the torsion angle.

It is necessary to emphasize that the results of the numerical calculations present approximate relations between the loading and the accepted parameter determining structure deformation. In fact, the obtained characteristics express the relationship between the torsion angle of the structure and the product: $\mathbf{M_{max} \cdot p_t}$, where $\mathbf{p_t}$ denotes a pseudo-time coefficient, as the step of load advantage application in the particular step of counts, whereas $\mathbf{M_{max}}$ is the maximum value of the structure loading. In the case considered, it is a maximum value of the torsional moment. The relationship is dependent on the accepted

method of the solution, the parameters of the iteration, and the shape of the equilibrium path between the products mentioned above and the actual loading of the numerical model. It should be noted that the loading of the numerical model is the maximum accepted value of the torsional moment for $\mathbf{p_t = 1}$.

2.3 Concluding remarks

On the basis of the numerical and experimental results several statements could be formulated, essential for engineering practice.

- The results obtained numerically show higher critical load values in all considered cases. It is possible that this can be explained by a rather imprecise rigidity reflecting the actual design in the numerical model as whole. It is related to the plate boundary conditions in particular. Additionally, the structure stiffness execution process should be considered.
- Establishing the back edge of the shell by limiting its degrees of freedom causes excessive stiffness in the numerical model of the structure. It is necessary to apply boundary conditions reproducing actual mount flexibility.
- The obtained divergence between the nonlinear numerical analysis and the results of the experiments suggests that appropriate imperfections of structure geometry in the numerical model should be taken into consideration. The effect would be the ability to propose reliable inferences, if not requirements, in relation to the technological process, particularly for neuralgic zones determining the load capacity of the structure.
- The presented study denotes experimental revision, information about structure behaviour under loading, and a verification function for the numerical FEM model in particular, where the solution of the problem requires nonlinear formulation.

3. Numerical and experimental analysis of torsined cylindrical shells reinforced with strenghten stringers

The subject of the second stage of research was a thin-walled open-section cylindrical shell stiffened by means of longitudinal stringers (Fig. 15), which model a zone with an extensive cutout (e.g. cockpit in an airframe structure). Such zones are usually joined with neighboring closed-section structural elements of cylindrical or slightly convergent shape. The planes of the joints determine boundary conditions eliminating the possibility of free deplanation of the outward sections.

A dimensioning form of load applied to the structure that, in the range of permissible load levels, can lead to loss of local stability of the shell, is the torsion retaining the character of a constrained one because of boundary conditions.

In order to determine the effect of longitudinal stiffening members on torsional rigidity within the full range of the analyzed deformations, structures with three, five and seven stringers were examined.

In the course of experimental work, photographic registration of subsequent deformation phases was carried out with simultaneous recording of vales of the torsion angle as the parameter enabling development of a representative equilibrium path. The tests were carried out both in sub-buckling range and in advanced post-buckling deformation states.

In order to determine the stress field in post-buckling deformation states that could constitute a basis for numerical analysis of the structure's fatigue life, a numerical model based on the finite elements method, for one of design solutions, was developed. The final

shape of the model was developed on the grounds of comparative analysis of deformation patterns and the nature of representative equilibrium paths that were obtained experimentally and numerically.

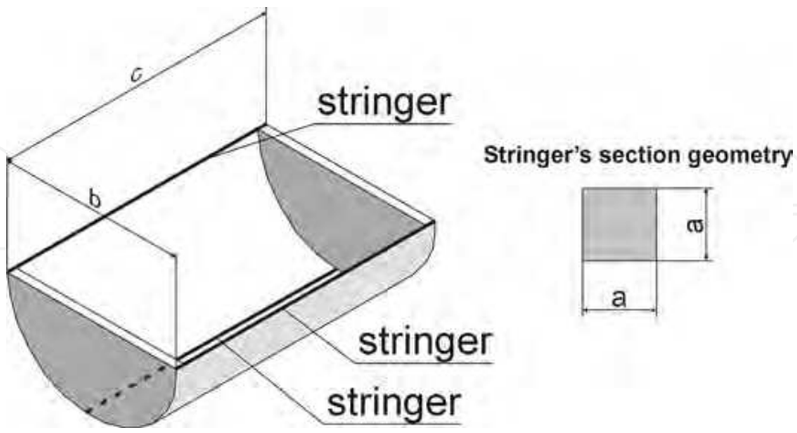

Fig. 15. Schematic geometry of the structure (a=10mm)

3.1 Experimental research

Three variants of the examined structure, differed by the number of stringers were used. In the first variant, the structure was reinforced with three stringers, in the second one — with five, and in the third variant — with seven stringers. To reproduce boundary conditions ensuring torsional rigidity of the structure corresponding to the constrained torsion, both end sections of the shell were provided with 20 mm plates. Schematic diagram of the experimental setup is shown in Fig. 16.

The structure was made of polycarbonate, for which the tensile strength test was carried out and material constants determined, i.e. Young's modulus E = 3000 MPa and Poisson ratio ν = 0.36.

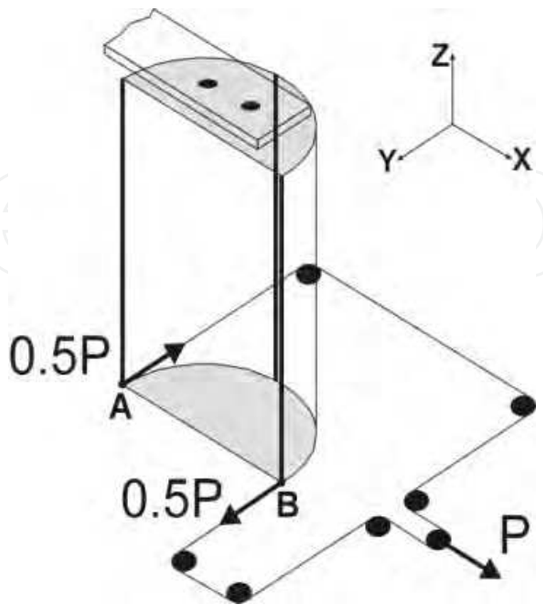

Fig. 16. Schematic diagram of the experimental setup

Fig. 17 shows the characteristic of the above-mentioned material corresponding to one-dimensional tensile stress. Clearly visible elastic and inelastic deformation zones suggest the possibility that the actual material characteristic can be approximated by an ideal elastic-plastic model. Moreover, because of low value of its elasticity modulus (by two orders of magnitude lower than that of steel) it was possible to carry out experiments at low values of external loads.

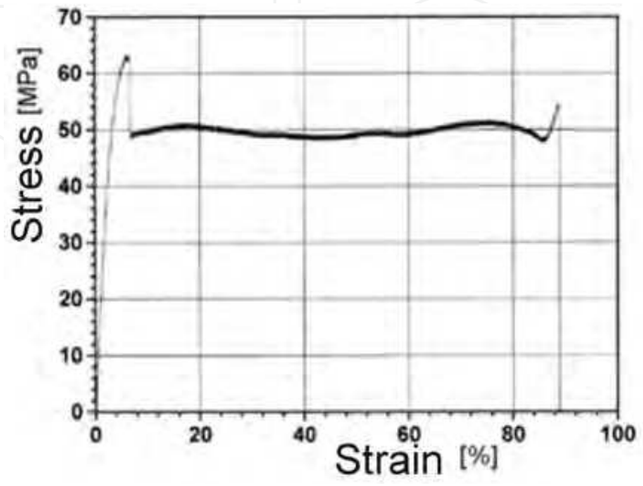

Fig. 17. Tensile stress plot for polycarbonate sample

The choice of the material, apart from the above-mentioned physical characteristics, was also justified by its high optical activity thanks to which it became possible to obtain qualitative information about optical effect distribution in circular polarization conditions. Joints between the shell and the stringers were realized by means of steel bolts spaced 20 mm apart. In order to avoid possible assembly stress at bolt joints, continuous observation of isochromatic fringe pattern fields in the vicinity of each bolt was performed throughout the whole assembly work. A view of the experimental stand with the model mounted on it is presented in Fig. 18a.

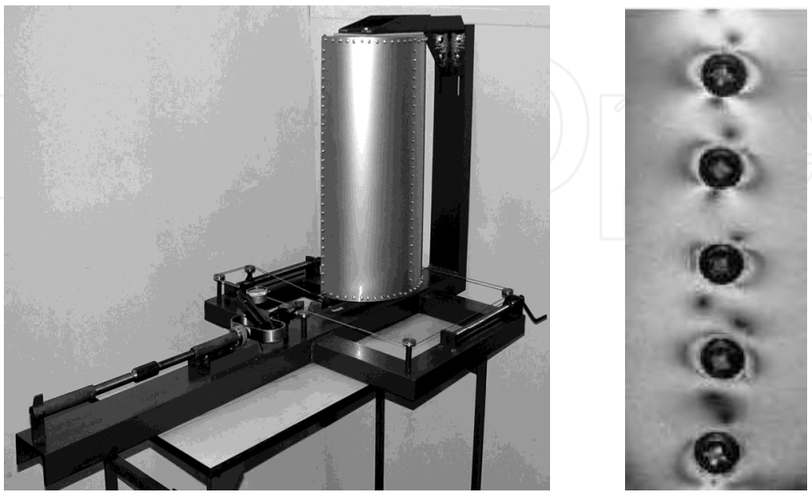

Fig. 18a. Experimental setup with the model fixed and ready for tests. 18b. Distribution of isochromatic fringe patterns in vicinity of bolts subject to control during assembly.

3.2 Structure reinforced with three stringers

The experimental work started with the structure reinforced by means of three stringers. The experiment was carried out with the load controlled by means of gravitational method ensuring good stability of load values. At the same time, one performed measurements of maximum values of the torsion angle. Based on these results, one determined a functional relationship between the twisting moment values and the model torsion angles representing an equilibrium path for a selected representative degree of freedom (cf. Fig. 22).

The first perceptible indications of loss of stability were observed in the vicinity of frames and external stringers, at the twisting moment value of $M_t \approx 20$ Nm, corresponding to torsion angle $\Theta \approx 2°$. While the load was increasing, the post-buckling equilibrium pattern covered larger and larger portion of the shell gradually reaching a global character.

It must be emphasized that the bifurcation-free character of the equilibrium path determined in the experiment was the result of the way in which the model was loaded and the possibility to perform the measurements only in steady-state conditions. Actually, the occurrence of large shell deformations and changes in their forms are connected with the jumps, in the course of which deformation increases although the load does not change. In fact, one deals here with a number of bifurcation processes, while the obtained equilibrium path represents the general character of dependence of the total torsion angle vs. twisting moment.

Fig. 19 presents an advanced form of post-buckling elastic deformation of the structure. The outward stringers were subject to significant deflection, while the central stringer did not change its original form. The obtained deformations confirm low torsional rigidity of the structure in advanced states, therefore it can be concluded that the use of solutions based on small number of stringers would be of little practical interest.

View from the inside. View from the outside.

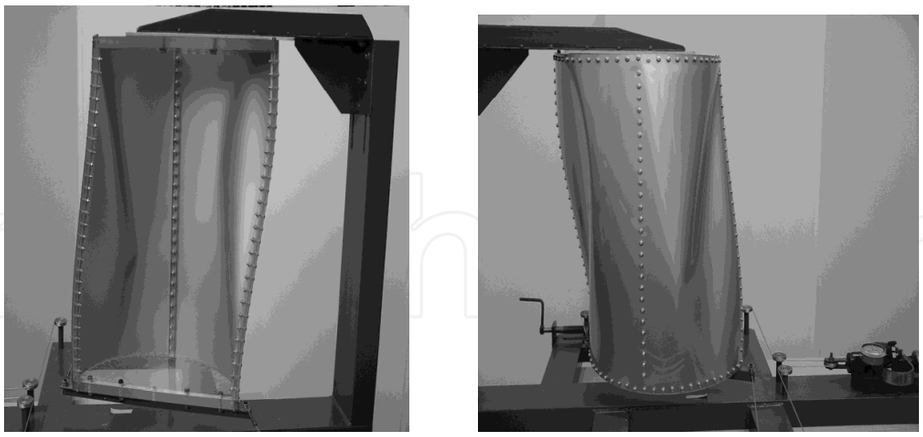

Fig. 19. Advanced post-buckling deformation, M_t = 60 Nm. M_t=60 Nm. (structure with three stringers)

3.3 Structure reinforced with five stringers

Another variant subject to examination represented a shell reinforced by means of five equally-separated stringers. The increase of the number of stringers was aimed at examining the expected increase of torsional rigidity, especially in advanced deformation states. As in

the previous variant, the result of the experiment consisted in developing a plot showing the relationship between the twisting moment and the structure's torsion angle (Fig. 22).

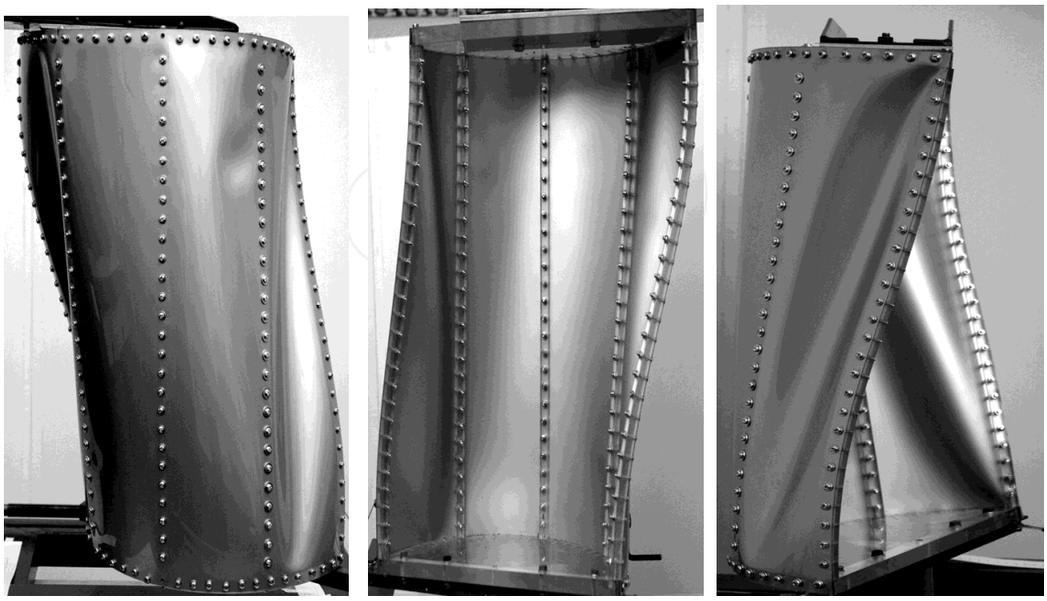

Fig. 20. Advanced post-buckling deformation phase (structure with 5 stringers), M_t = 75 Nm.

The representative equilibrium path shows that loss of stability occurred here in a way similar to that observed in the case of structure with three stringers. The presence of additional stringers placed between the outward ones and the central member (Fig.20) did not have any significant effect on rigidity of the examined structure.

3.4 Structure reinforced with seven stringers

The increase of the number of stringers to seven resulted in a significant increase of torsional rigidity of the structure. A considerable change was observed in the form in which the shell was loosing its stability, consisting in distinct increase of load on the stringers. The relationship of the structure's torsion angle vs. the twisting moment obtained in the course of experiment is shown in Fig. 22. Post-buckling deformation patterns are presented in Figs. 21. The process of local buckling was initiated in the vincinity of boundary stringers at twisting moment value of M_t = 33 Nm. Deformation of the shell proceeded smoothly. The experiment ended after the twisting moment reached M_t = 110 Nm. It was found that largest deformations occurred in two outermost segments adjacent to the shell edges. The presence of additional stringers resulted in a decrease of the depth of the folds which, in fact, ment an increase of the system's torsional rigidity. Deformations of the shell and stringers in the central part of the structure remained small compared to the deformations observed in the first two variants.

Fig. 22 presents a comparison of three characteristics corresponding to the three analyzed solutions of the structure design. In comparison with the first two variants, the structure reinforced with seven stringers revealed a significant increase of torsional rigidity. For instance, at twisting moment value M_t = 55 Nm, the torsion angle of the structure with three stringers amounted to 20° compared to only about 6° in the case of the third variant. The applied reinforcement shows therefore significant effect on the increase of torsional rigidity as well as on the values and patterns of stress distribution in the structure.

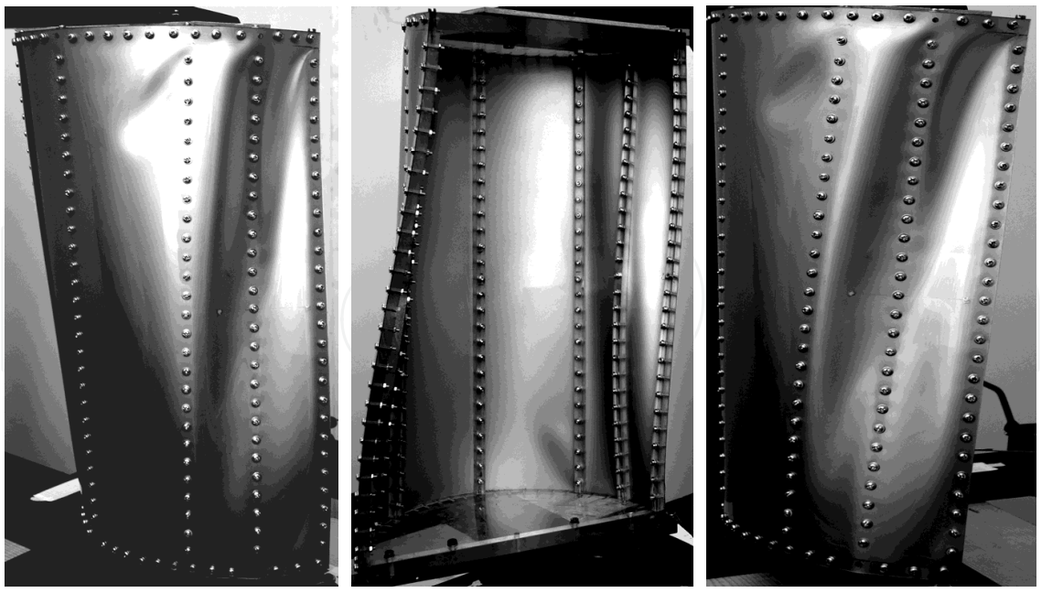

Fig. 21. Advanced post-buckling deformation pattern (structure with 7 stringers), M_t=110 Nm

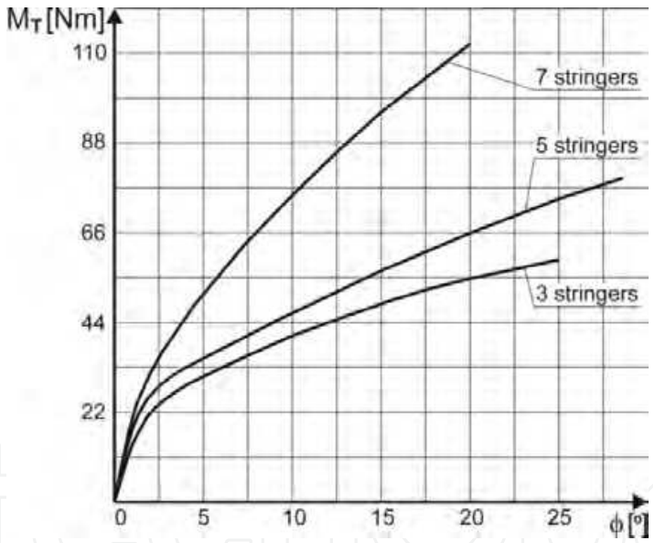

Fig. 22. Comparison of representative equilibrium paths.

3.5 Examination by means of optical polarization methods

Optical sensivity of the material of which the test structure was constructed allowed for observation of distributions of optical effects in polarized light. In the case of bending/membrane state occurring in post-buckling deformation conditions, the optical effect observed in circularly-polarized light can not be identified with isochromatic fringe patterns as the principal stress axes can vary along the shell thickness.

These effects are overestimated compared to isochromatic fringe pattern values, and the degree of overestimation increases with the increasing angle between the directions of principal stressesof bending and membrane states.

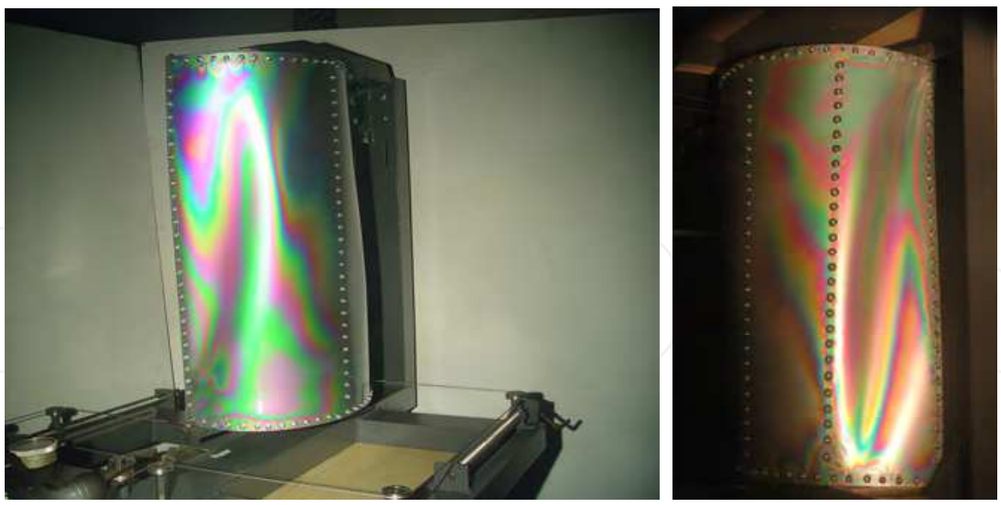

Fig. 23. Optical effect distributions: a model with 3 stringers (left), a model with 5 stringers (right)

The quantitative analyses of the observed patterns can be biased with a significant error. Nevertheless, the observed optical effects represent a source of vital information useful in determination of high stress gradients zones that can then be particularly helpful when developing a numerical model aimed at determination of stress fields characteristic for advanced post-buckling deformation states.
Figs. 23–24 present an example distributions of optical effects observed in the examined models are.

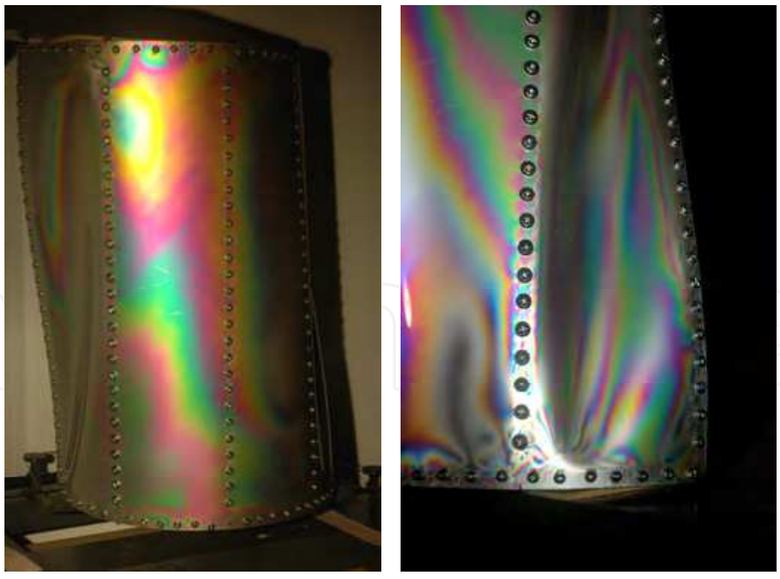

Fig. 24. Optical effect distributions — a model with 5 stringers

3.6 Nonlinear numerical analysis

In the considered issue, one accepted the maximum values of torsion angle of the structure and the twisting moment of a couple of the forces, acting on the frame closing the boundary

section as representative parameters for determining the equilibrium path. As a base of the analysis process, one applied the Newton – Raphson method and the corrective strategy based on arc-length control concept formulated by Riks – Wempner. The attempts to apply the Newton – Raphson method with the basic correction phase, did not allow for obtaining a convergent solution. Reliability of the obtained results was assessed by comparing the equilibrium path to the result of experiment, as well as assessing the compatibility of deformations obtained in the numerical way and those obtained experimentally. Information from both of these comparisons suggesting the necessity of making multiple corrections in the numerical models. Creating those models, one took into consideration a number of factors resulting from the necessity to retain some features of the real structure. Most important was to use a correct set of finite elements to make an appropriate simplifications in the geometry of the modeled structure and to appropriate reproduce the boundary conditions. In order to meet the above requirements, it was necessary to perform a number of numerical tests. Fig 25 illustrates the concept of boundary conditions reproduction, according to which the nodes fixing the structure are represented by two constraint points with blocked translational and rotational degrees of freedom. This corresponds to the real manner of fixing the structure by means of two bolts fastening one of the outward frames to the test stand.

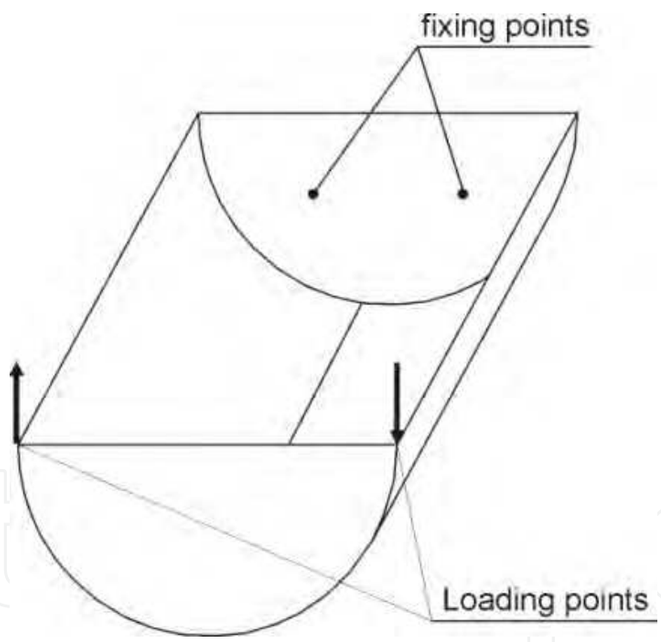

Fig. 25. Schematic diagram of model fix and load

Nonlinear numerical analyses were performed using the MSC MARC-2007 software package. Several model versions of the structure, with three stringers, and with various ways of reproduction of stringers and their joints with the shell were created.
In all cases, the shell was modeled using a bilinear, thin-shell element. The frames, and in some cases the stringers, were modeled using bilinear, four-node thick-shell element with global displacement and rotations as the degree of freedom. Bilinear interpolation was used for the coordinates, displacement and the rotations. The six degrees of freedom per node are as follows:

u, v, w - displacement components defined in global Cartesian x,y,z – coordinate system,
Φ_x, Φ_y, Φ_z - rotation components about global: **x, y, z** – axis respectively.
In order to reproduce the structure stiffness ensuring compatibility with experiment results, three kinds of elements were applied for the modeling stringers: bilinear thick-shell element, elastic beam element and three-dimensional arbitrary-distorted brick elements.
Elastic beam with transverse shear is a straight beam in space which includes transverse shear effects with elastic material response. Linear interpolation is used for the axial and the transverse displacements as well as for the rotations. Section forces are output as: the axial force, local $\mathbf{T_x}$, $\mathbf{T_y}$ - shear forces, bending moments about the **x, y** – axes of the cross section respectively, torque moment about the beam axis.
The three-dimensional arbitrary-distorted brick element is an eight-node, isoparametric, arbitrary hexahedral. As this element uses trilinear interpolation functions, the strains tend to be constant throughout the element. The element can be used for all the constitutive relations. There are three global degrees of freedom: u, v, w – at each node.
In the one of the models, joints between stringers and the shell were reproduced in a discrete way, by means of beam-type elements, with simultaneous use of contact preventing elements interpenetrate in advanced deformation states. In other cases, joints of continuous kind were used. The results of calculation show that the way in which the joints between shell and stringers were modeled, had little influence on the character of effective stress distribution in the structure shell. Moreover, the model with discrete joints is characterized by high complexity, which – as it was proved in numerical tests – makes the convergence of nonlinear analyses much more difficult to obtain and leads to deformation patterns incompatible with those obtained in the experimental way in the post-buckling range.
Fig. 26 presents comparison of effective stress distribution according to Huber-Mises-Hencky criterion in the pre-buckling range, for the models with stringers constructed of 3D elements and joints realized by means of two different methods.

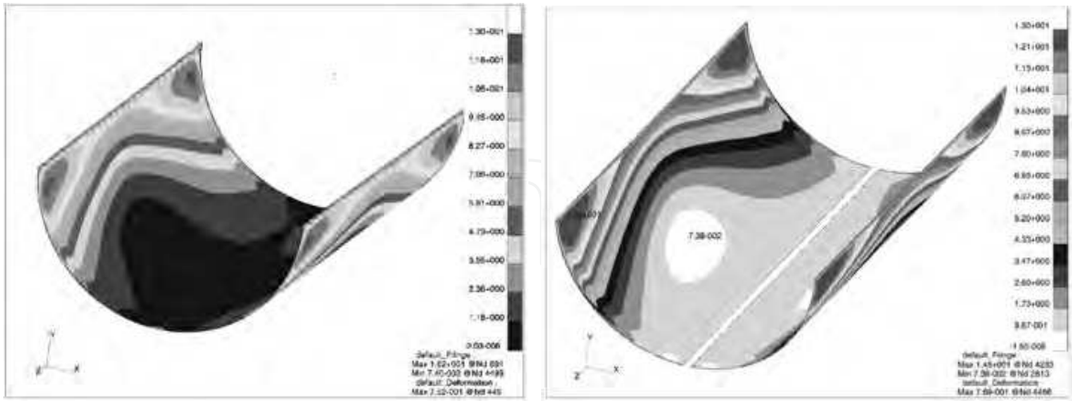

Fig. 26. Comparison of stress distributions in the middle layer according to Mises' hypothesis obtained for the discrete joints model (left) and the continuous joints model (right)

Conformity of deformations was obtained for two version of the models, with continuous joints. In the first one, the stringers made of three-dimensional elements were used. In the second case, one applied one-dimensional stringers, made of beam-type elements.

Comparison of the calculated deformation patterns corresponding to maximum load with the deformation observed in the course of experimental investigation is presented in Fig. 27. For both models, the equilibrium paths representing the relationship of twisting moment vs. torsion angle, complied with the similar ones, measured experimentally. The comparison of equilibrium paths obtained by means of numerical calculations with the results of experiment is presented in Fig. 28.
By comparing the values of the representative state parameter (torsion angle) pertaining to specific values of the control parameter (twisting moment) one can conclude that the maximum divergence between results obtained numerically with those measured in the experiment for the highest applied loads amounts to about 30%.

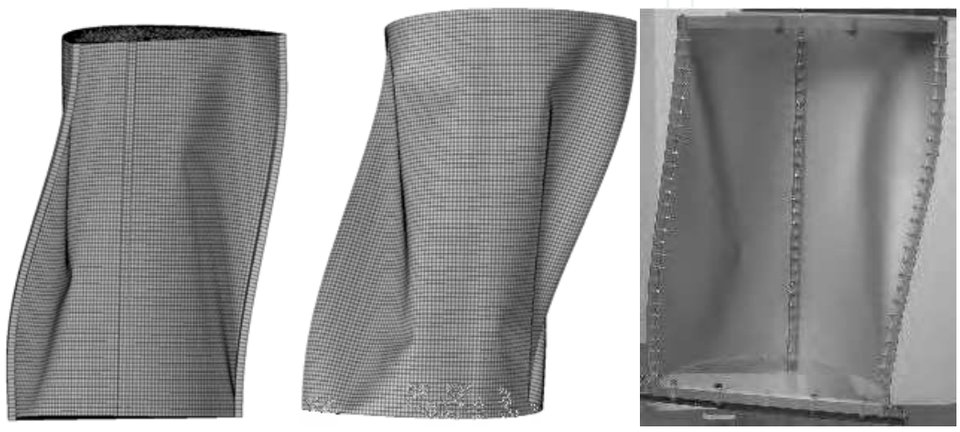

a) b) c)

Fig. 27. Post-buckling deformation patterns under the same load:
(a) a model with stringers made of 3D elements;
(b) a model with stringers made of beam elements;
(c) actual structure under load

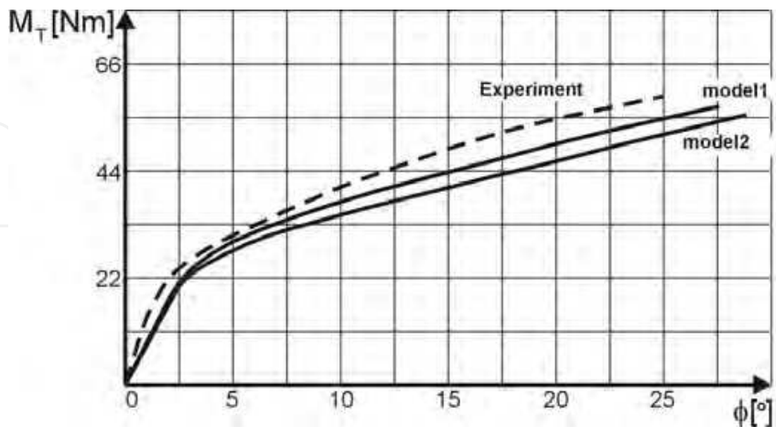

Fig. 28. Comparison of representative equilibrium paths: model1 — stringers of 3D elements; model2 — stringers of beam elements

As it follows from the above comparison of the characteristics, the model reproducing stiffness of stringers based on 3D elements shows better conformity with experiment than

the model based on beam elements. The obtained convergence of equilibrium paths and deformation patterns allows to conclude that stress distributions obtained as the result of numerical analyses are close to the actual ones, and therefore can be adopted as a basis for estimates concerning durability of the structure. Fig. 29 and 30 present comparison of stress distributions according to Huber-Mises-Hencky hypothesis for different deformation phases. The analysis of that juxtaposition leads to the conclusion that in the post-buckling deformations phase some significant redistribution of stresses occur, and therefore the use of simplified calculation algorithms based on linearized analysis of stability has no grounds in the case of structures of that type.

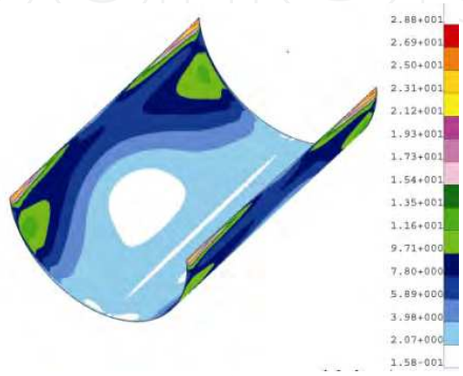

a)

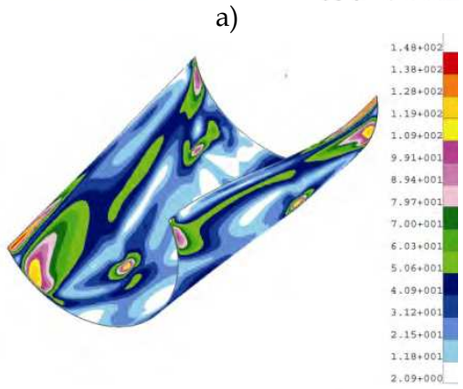

b)

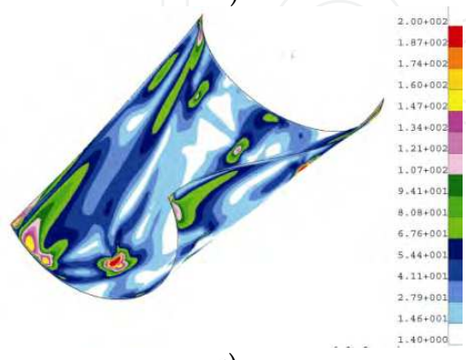

c)

Fig. 29. Stress distributions according to Mises' hypothesis: (a model with stringers represented by beam elements) a) 25% load — middle layer; b) 70% load — middle layer; c) 100% load — middle layer

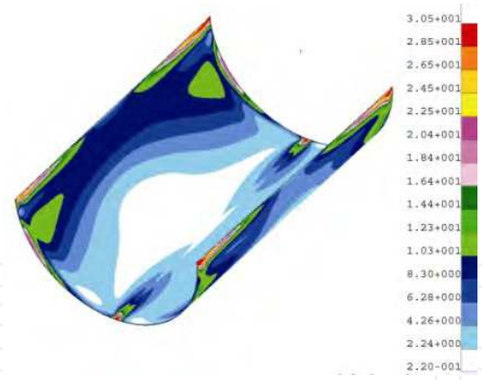

d)

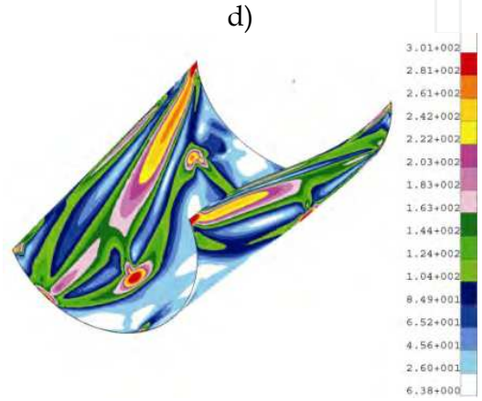

e)

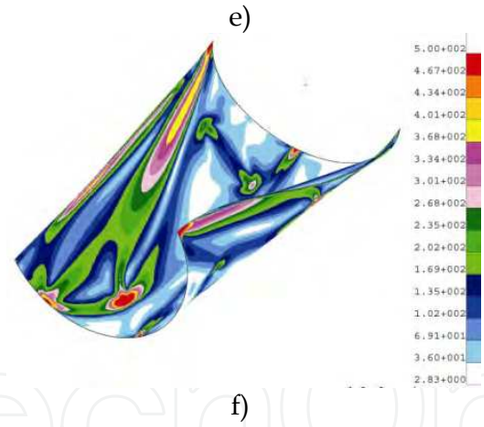

f)

Fig. 30. Stress distributions according to Mises' hypothesis: (a model with stringers represented by beam elements): d) 25% load — external layer; e) 70% load — external layer; f) 100% load — external layer.

After suitable comparison, the satisfactory similarity between isochromatic fringe pattern distribution in the experimental model and the stress distribution according to Mises' hypothesis in numerical model was found (Fig. 31). It allowed to accept numerically obtained results as reliable.

At the next step, nonlinear numerical calculations of models reinforced with five and seven stringers were carried out. Creating FEM models, one retained identical boundary conditions as described above. All analyses based on the same prediction methods and correction strategies as in case of the structure with three stringers.

Fig. 31. Comparison of isochromatic fringe pattern distribution in the experimental model with stress distribution according to Mises' hypothesis — model with three stringers

Fig. 32 and 33 present comparisons of deformations obtained during experiments with suitable results of nonlinear numerical calculations, for the same value of twisting moment (80% of the maximum). Representative equilibrium paths are presented on Fig. 28.

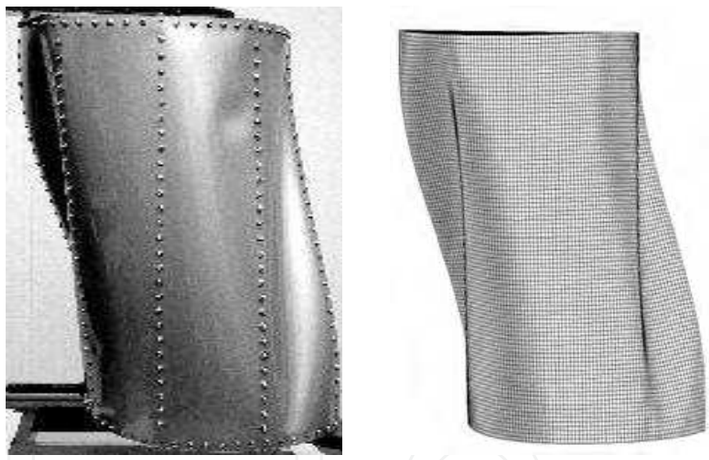

Fig. 32. Structure reinforced by 5 stringers – comparison of deformation forms obtained as the result of experiment (left) and nonlinear numerical analysis (right) – stringers reproduced with beam elements

3.7 Concluding remarks

The performed numerical analyses and experimental investigation lead to several conclusions of, how it seems, cognitive and utilitarian significance.

- The concept of performing the numerical analyses associated with experiment refers to the observed tendency, according to which the contemporary design of load-carrying structures, should be supported by permanent improvement of numerical formulations. The common feature of the two approaches to structure design is idealization of structures. We have in mind that, in engineering applications, the FEM is an approximate method and the received results refers not to the real structure, but to an

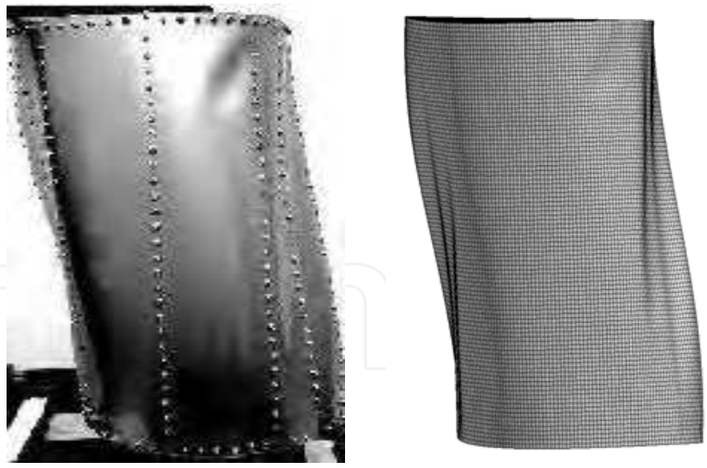

Fig. 33. Structure reinforced by 7 stringers – comparison of deformation forms obtained as the result of experiment (left) and nonlinear numerical analysis (right) – stringers reproduced with brick elements

idealized model. So that, without denying the importance of non-linear numerical analyses as tools of unquestionable effectiveness, we must keep in mind the problem of unreliability of results. It seems then that experimental verifications of FEM analyses is justified and sometimes indispensable. Such verification significantly increases reliability of results obtained on the numerical way.

- Despite the limitations connected with the possibilities of proper interpretation of optical effects, analyzed in terms of quality considerations, the results of photo-elastic examinations may provide the significant information about the existence of stress concentration areas in pre-buckling and post-buckling states, even before numerical models are created.
- The results of experimental investigation used for improving numerical models and for correcting computing procedures, pointed the necessity of taking into consideration the corrective phase of nonlinear analysis. Neglecting this phase leads to incompatibilities of numerical and experimental results or may resort in the lack of convergence of the solution.
- It is necessary to emphasize that compatibility of deformations in experimental and numerical models validated the credibility of stress fields received as the result of numerical computation.
- There are some other, more detailed remarks and conclusions that follow on the suggested procedure. For example, the results of numerical analyses and experimental examinations proved, that the method of modeling of connections between the stringers and the shell did not have any significant effect on the character of global deformation. It is also important to notice that the model based on stringers fixed with discrete connections to the shell, which has great complexity, makes it more difficult to obtain a convergent solution in the non-linear analysis.

4. References

Andrianov J., Awrejcewicz J., Manewitch L.I. (2004) *Asymptotical Mechanics of thin-walled structures.* Springer, Berlin, Germany

Awrejcewicz J., Krysko A. (2003) *Nonclassical thermoelastic problems in nonlinear dynamics of shells.* Springer, Berlin, Germany

Awrejcewicz J., Krysko V.A., Vakakis A.F. (2004) N*onlinear dynamics of continuous elastic systems.* Springer, Berlin, Germany

Arborcz J. (1985). *Post-buckling behavior of structures. Numerical techniques for more complicated structures.* Lecture Notes In Physics, 228, USA

Bathe K.J. (1996). *Finite element procedures*, Prentice Hall, USA

Doyle J.F. (2001). *Nonlinear analysis of thin-walled structures.* Springer-Verlag, Berlin, Germany

Felippa C. A. (1976): *Procedures for computer analysis of large nonlinear structural system in large engineering systems.* ed. by A. Wexler, Pergamon Press, London, UK

Kopecki T. (2010). *Advanced deformation states in thin-walled load-bearing structure design work.* Oficyna Wydawnicza Politechniki Rzeszowskiej, Rzeszów, Poland

Lynch C., Murphy A., Price M., Gibson A. (2004). *The computational post buckling analysis of fuselage stiffened panels loaded in compression.* Thin-Walled Structures, 42:1445-1464, USA

Marcinowski J. (1999). *Nonlinear stability of elastic shells*. Oficyna Wydawnicza Politechniki Wrocławskiej, Wrocław, Poland

Mohri F., Azrar L., Potier-Ferry M. (2002). *Lateral post buckling analysis of thin-walled open section beams*. Thin-Walled Structures, 40:1013-1036, USA

Niu M. C. (1988). *Airframe structural design.* Conmilit Press Ltd., Hong Kong

Rakowski G., Kacprzyk Z. (2005). *Finite elements method in structure mechanics.* Oficyna Wydawnicza Politechniki Warszawskiej, Warszawa, Poland

Ramm E. (1987). *The Riks/Wempner Approach – An extension of the displacement control method in nonlinear analysis*. Pineridge Press, Swensea, UK

Aben H. (1979). *Integrated photoelasticity.* Mc Graw-Hill Book Co., London, UK

IntechOpen

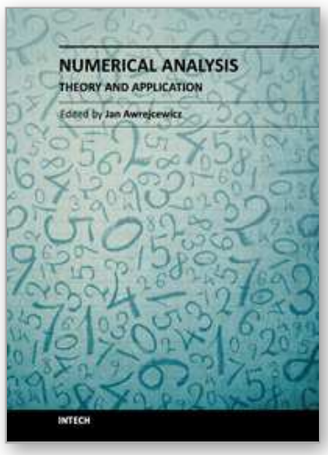

Numerical Analysis - Theory and Application

Edited by Prof. Jan Awrejcewicz

ISBN 978-953-307-389-7
Hard cover, 626 pages
Publisher InTech
Published online 09, September, 2011
Published in print edition September, 2011

Numerical Analysis â€“ Theory and Application is an edited book divided into two parts: Part I devoted to Theory, and Part II dealing with Application. The presented book is focused on introducing theoretical approaches of numerical analysis as well as applications of various numerical methods to either study or solving numerous theoretical and engineering problems. Since a large number of pure theoretical research is proposed as well as a large amount of applications oriented numerical simulation results are given, the book can be useful for both theoretical and applied research aimed on numerical simulations. In addition, in many cases the presented approaches can be applied directly either by theoreticians or engineers.

How to reference

In order to correctly reference this scholarly work, feel free to copy and paste the following:

Tomasz Kopecki (2011). Coupling Experiment and Nonlinear Numerical Analysis in the Study of Post-Buckling Response of Thin-Walled Airframe Structures, Numerical Analysis - Theory and Application, Prof. Jan Awrejcewicz (Ed.), ISBN: 978-953-307-389-7, InTech, Available from: http://www.intechopen.com/books/numerical-analysis-theory-and-application/coupling-experiment-and-nonlinear-numerical-analysis-in-the-study-of-post-buckling-response-of-thin-

INTECH
open science | open minds

InTech Europe
University Campus STeP Ri
Slavka Krautzeka 83/A
51000 Rijeka, Croatia
Phone: +385 (51) 770 447
Fax: +385 (51) 686 166
www.intechopen.com

InTech China
Unit 405, Office Block, Hotel Equatorial Shanghai
No.65, Yan An Road (West), Shanghai, 200040, China
中国上海市延安西路65号上海国际贵都大饭店办公楼405单元
Phone: +86-21-62489820
Fax: +86-21-62489821

© 2011 The Author(s). Licensee IntechOpen. This chapter is distributed under the terms of the Creative Commons Attribution-NonCommercial-ShareAlike-3.0 License, which permits use, distribution and reproduction for non-commercial purposes, provided the original is properly cited and derivative works building on this content are distributed under the same license.

IntechOpen

IntechOpen